

Buckling of simply supported thin plate with variable thickness under bi-axial compression using perturbation technique

Haigui Fan^{*1}, Zhiping Chen², Zewu Wang¹ and Peiqi Liu¹

¹School of Chemical Machinery and Safety Engineering, Dalian University of Technology,
No.2 Linggong Road, Dalian, Liaoning 116023, P.R. China

²Institute of Process Equipment, Zhejiang University, 38 Zheda Road, Hangzhou, Zhejiang 310027, P.R. China

(Received January 13, 2019, Revised March 2, 2019, Accepted March 5, 2019)

Abstract. An analytical research on buckling of simply supported thin plate with variable thickness under bi-axial compression is presented in this paper. Combining the perturbation technique, Fourier series expansion and Galerkin methods, the linear governing differential equation of the plate with arbitrary thickness variation under bi-axial compression is solved and the analytical expression of the critical buckling load is obtained. Based on that, numerical analysis is carried out for the plates with different thickness variation forms and aspect ratios under different bi-axial compressions. Four different thickness variation forms including linear, parabolic, stepped and trigonometric have been considered in this paper. The calculated critical buckling loads and buckling modes are presented and compared with the published results in the tables and figures. It shows that the analytical expressions derived by the theoretical method in this paper can be effectively used for buckling analysis of simply supported thin plates with arbitrary thickness variation, especially for the stepped thickness that used in engineering widely.

Keywords: buckling; thin plate; thickness variation; compression; analytical expressions

1. Introduction

Thin plates with variable thickness are widely used in civil, aerospace and marine structures. They possess a number of attractive features, such as material saving, weight reduction, stiffness enhancing and high strength to weight ratio. Consideration of buckling behavior for such plates is essential to have an efficient and reliable design. Research on buckling of thin plate with variable thickness under compression has gained more and more attention in recent years.

Wittrick and Ellen (1962) pioneered analytical research on buckling of rectangular plates with linear and exponential variation in thickness in one direction using the Galerkin method. Applying a perturbation technique, the critical buckling stress of a simply supported rectangular plate with general thickness was derived by Chenil and Dua (1973). The results obtained for a plate with linear variation in thickness are in good agreement with those of Wittrick and Ellen (1962). Navaneethakrishnan (1988) solved the differential equation characterizing the transverse deflection of a thin rectangular plate of variable thickness semi-numerically using the quintic spline collocation technique. The buckling coefficients and the mode shapes were obtained for different boundary conditions. Nerantzaki and Katsikadelis (1996) presented the analog equation method to analyze buckling of plates with variable thickness. The eigenvalue problem for a differential equation of buckling

was converted into a linear problem and the buckling loads were established numerically then. The extended Kantorovich method in conjunction with the exact element method were used by Eisenberger and Alexandrov (2003) to obtain buckling loads and buckling modes of rectangular thin plates with thickness that varies in the directions parallel to the two sides. Saeidifar *et al.* (2010) introduced a numerical calculation of buckling loads for an elastic rectangular plate with variable thickness and elasticity modulus in one direction by transforming the governing partial differential equation of plate motion to an ordinary differential equation. Buckling analysis of thin rectangular plates under uniaxial and bi-axial locally distributed compressive stresses was performed analytically by Wang *et al.* (2016) using the differential quadrature method. Li *et al.* (2018) and Wang *et al.* (2016) used distinctive symplectic superposition method to solve buckling problem of plates with fully free edges and combined clamped and simply supported edges under bi-axial compression. The analytic solutions and mode shapes were presented and validated by the finite element method. Minh *et al.* (2018) used phase field method to investigate stability of cracked rectangular FGM plate with linear variable thickness. It showed that the thickness variation had greater influence on buckling behavior of the plate than the cracks. As a typical thickness variation form, buckling behavior of stepped rectangular plate has attracted much attention. Kobayashi and Sonoda (1990) developed a power series method to solve the buckling problem of uniaxially compressed rectangular plates with stepped thickness. The effects of thickness variation, plate aspect ratios and boundary conditions on the buckling load were analyzed. Based on

*Corresponding author, Ph.D.
E-mail: haigui@dlut.edu.cn

the Kirchhoff plate theory, Xiang and Wang (2002) and Xiang and Wei (2004) presented the buckling loads of multi-stepped rectangular plates by the Levy method and state-space technique. Effects of step-number, step-thickness, step-length and the boundary conditions on buckling behavior of the plate were analyzed. Local buckling and post-buckling behavior of stepped plates with different geometries were studied by Azhari *et al.* (2005). The buckling loads and lateral displacements for the plates subjected to uniaxial and bi-axial compressions were obtained. Wilson and Rajasekaran (2013, 2014) and Rajasekaran and Wilson (2013) applied the finite difference method to research buckling load of stepped rectangular thin plate with different boundary conditions under different force combinations. New and exact buckling results corresponding to different geometries of the plates were presented and analyzed. In addition, investigations on tanks with stepped thickness by Chen *et al.* (2012) and Gong *et al.* (2013) are also worth reference.

In this paper, an analytical method based on perturbation technique and Fourier series expansion is established to obtain buckling load of simply supported rectangular thin plate with arbitrary thickness variation along both x and y directions under bi-axial compression. Different thickness variations of the plate such as linear, parabolic, stepped and trigonometric forms are researched under different combinations of compression. The buckling loads and buckling modes for different cases are calculated and the effects of thickness variation, aspect ratio and compression combination on the buckling coefficients are discussed based on numerical analyses. Comparative studies are also performed to verify the presented method in this paper.

2. Analytical solution of the buckling load

Consider the thin rectangular plate under bi-axial compression as shown in Fig. 1. The length and width are a and b respectively and the thickness h varies in x and y directions arbitrarily. According to the classical plate theory, the governing equation of the plate under forces can be expressed as Eq. (1).

$$\frac{\partial^2 M_x}{\partial x^2} + 2\frac{\partial^2 M_{xy}}{\partial x \partial y} + \frac{\partial^2 M_y}{\partial y^2} + N_x \frac{\partial^2 W}{\partial x^2} + 2N_{xy} \frac{\partial^2 W}{\partial x \partial y} + N_y \frac{\partial^2 W}{\partial y^2} = 0 \quad (1)$$

in which W is the lateral deformation, N_x , N_y and N_{xy} are the in-plane forces per unit length, M_x , M_y and M_{xy} are moment components which satisfy

$$\begin{aligned} M_x &= -D \left(\frac{\partial^2 W}{\partial x^2} + \nu \frac{\partial^2 W}{\partial y^2} \right), \quad M_{xy} = -D(1-\nu) \left(\frac{\partial^2 W}{\partial x \partial y} \right), \\ M_y &= -D \left(\frac{\partial^2 W}{\partial y^2} + \nu \frac{\partial^2 W}{\partial x^2} \right) \end{aligned} \quad (2)$$

where $D = Eh^3/12(1-\nu^2)$.

Since the plate is considered compressed by bi-axial loads alone in this paper as shown in Fig. 1, the axial force components will satisfy $N_x = -p$, $N_y = -q$ and the shear force component will satisfy $N_{xy} = 0$. Then, Eq. (1) can be transformed as follows

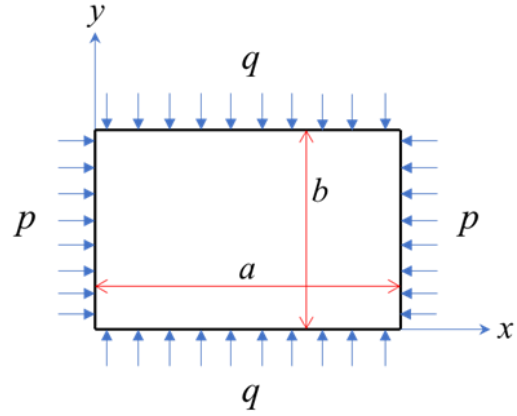


Fig. 1 Rectangular plate under bi-axial compression

$$\begin{aligned} & \frac{Eh^3}{12(1-\nu^2)} \nabla^2 \nabla^2 W + \frac{6Eh^2}{12(1-\nu^2)} \left(\frac{\partial h}{\partial x} \frac{\partial}{\partial x} \nabla^2 W + \frac{\partial h}{\partial y} \frac{\partial}{\partial y} \nabla^2 W \right) \\ & + \frac{3Eh}{12(1-\nu^2)} \left(\frac{\partial^2 W}{\partial x^2} + \nu \frac{\partial^2 W}{\partial y^2} \right) \left[h \frac{\partial^2 h}{\partial x^2} + 2 \left(\frac{\partial h}{\partial x} \right)^2 \right] \\ & + \frac{3Eh}{12(1-\nu^2)} \left(\frac{\partial^2 W}{\partial y^2} + \nu \frac{\partial^2 W}{\partial x^2} \right) \left[h \frac{\partial^2 h}{\partial y^2} + 2 \left(\frac{\partial h}{\partial y} \right)^2 \right] \\ & + \frac{6(1-\nu)Eh}{12(1-\nu^2)} \frac{\partial^2 W}{\partial x \partial y} \left(h \frac{\partial^2 h}{\partial x \partial y} + 2 \frac{\partial h}{\partial x} \frac{\partial h}{\partial y} \right) + p \frac{\partial^2 W}{\partial x^2} + q \frac{\partial^2 W}{\partial y^2} = 0 \end{aligned} \quad (3)$$

In order to make the solutions more general, the following non-dimensional parameters are introduced

$$\xi = \frac{x}{a}, \quad \eta = \frac{y}{b}, \quad w = \frac{W}{h_0}, \quad H = \frac{h}{h_0} \quad (4)$$

where h_0 is the nominal thickness of the plate.

In view of the non-dimensional parameters, the governing differential equation can be transformed by substituting Eq. (4) into Eq. (3) to yield

$$\begin{aligned} & H^3 \left(\frac{\partial^4 w}{\partial \xi^4} + 2 \frac{a^2}{b^2} \frac{\partial^4 w}{\partial \xi^2 \partial \eta^2} + \frac{a^4}{b^4} \frac{\partial^4 w}{\partial \eta^4} \right) + 6H^2 \frac{\partial H}{\partial \xi} \frac{\partial}{\partial \xi} \left(\frac{\partial^2 w}{\partial \xi^2} + \frac{a^2}{b^2} \frac{\partial^2 w}{\partial \eta^2} \right) \\ & + 6 \frac{a^2}{b^2} H^2 \frac{\partial H}{\partial \eta} \frac{\partial}{\partial \eta} \left(\frac{\partial^2 w}{\partial \xi^2} + \frac{a^2}{b^2} \frac{\partial^2 w}{\partial \eta^2} \right) + 3H^2 \frac{\partial^2 H}{\partial \xi^2} \left(\frac{\partial^2 w}{\partial \xi^2} + \nu \frac{a^2}{b^2} \frac{\partial^2 w}{\partial \eta^2} \right) \\ & + 6H \frac{\partial H}{\partial \xi} \frac{\partial H}{\partial \xi} \left(\frac{\partial^2 w}{\partial \xi^2} + \nu \frac{a^2}{b^2} \frac{\partial^2 w}{\partial \eta^2} \right) + 3 \frac{a^2}{b^2} H^2 \frac{\partial^2 H}{\partial \eta^2} \left(\frac{a^2}{b^2} \frac{\partial^2 w}{\partial \eta^2} + \nu \frac{\partial^2 w}{\partial \xi^2} \right) \\ & + 6 \frac{a^2}{b^2} H \frac{\partial H}{\partial \eta} \frac{\partial H}{\partial \eta} \left(\frac{a^2}{b^2} \frac{\partial^2 w}{\partial \eta^2} + \nu \frac{\partial^2 w}{\partial \xi^2} \right) + 6(1-\nu) \frac{a^2}{b^2} H^2 \frac{\partial^2 H}{\partial \xi \partial \eta} \frac{\partial^2 w}{\partial \xi \partial \eta} \\ & + 12(1-\nu) \frac{a^2}{b^2} H \frac{\partial H}{\partial \xi} \frac{\partial H}{\partial \eta} \frac{\partial^2 w}{\partial \xi \partial \eta} + \frac{pa^2}{D_0} \frac{\partial^2 w}{\partial \xi^2} + \frac{qb^2}{D_0} \frac{\partial^2 w}{\partial \eta^2} = 0 \end{aligned} \quad (5)$$

A non-dimensional parameter λ representing the ratio of compression along x coordinate to that along y coordinate is introduced as follows

$$q = \lambda p \quad (6)$$

As we know that various thickness variations such as trigonometric, linear, exponential and stepped forms are used in thin plate structures. Since some thickness variations may be too complicated to be applied in Eq. (5)

directly, the buckling parameters may not be analytically solved or expressed as analytical formulas. Thus, the perturbation method is applied in this paper and the thickness function that varies arbitrarily in the x and y coordinates is assumed to take on the following form

$$h(x, y) = h_0 + \varepsilon h_1(x, y) + \varepsilon^2 h_2(x, y) + \dots = h_0 + \sum_{i=1}^{\infty} \varepsilon^i h_i(x, y) \quad (7)$$

where $\varepsilon(0 \leq \varepsilon \leq 1)$ is the non-dimensional parameter indicating the thickness variation magnitude, h_0 is the nominal thickness and $h_i(i \geq 1)$ denotes specific thickness variation function that determines the real thickness of the plate.

Using the perturbation method, difficulties of applying complicated variable thickness expression directly in the solution process can be avoided and the buckling load for the rectangular plate with arbitrary thickness variation can be solved analytically. According to Eq. (4), the thickness function as shown in Eq. (7) can be transformed into a non-dimensional form

$$H(\xi, \eta) = 1 + \varepsilon H_1(\xi, \eta) + \varepsilon^2 H_2(\xi, \eta) + \dots = 1 + \sum_{i=1}^{\infty} \varepsilon^i H_i(\xi, \eta) \quad (8)$$

According to the perturbation method, the non-dimensional lateral displacement will be expressed as follows

$$\begin{aligned} w(\xi, \eta) &= w_0(\xi, \eta) + \varepsilon w_1(\xi, \eta) + \varepsilon^2 w_2(\xi, \eta) + \dots \\ &= w_0(\xi, \eta) + \sum_{i=1}^{\infty} \varepsilon^i w_i(\xi, \eta) \end{aligned} \quad (9)$$

in which w_0 represents the solution corresponding to nominal thickness h_0 , w_i represents the variation of lateral displacement caused by specific thickness variation function h_i .

The rectangular plate is assumed as simply supported at all edges in this paper. Because for the other boundary conditions like clamped supported or free, the plate's displacement satisfying the boundary conditions are too complicated to be expressed analytically. It leads to the failure to derive the analytical formula of the critical buckling load using this method. Thus, the fully simply supported condition is considered in this paper and the boundary condition can be expressed as follows

$$w|_{\xi=0,1} = 0 \quad w|_{\eta=0,1} = 0 \quad \left. \frac{\partial^2 w}{\partial \xi^2} \right|_{\xi=0,1} = 0 \quad \left. \frac{\partial^2 w}{\partial \eta^2} \right|_{\eta=0,1} = 0 \quad (10)$$

In order to arrive at the critical buckling load of the plate under bi-axial compression, the pressure acting on the plate along x coordinate will be expressed in term of ε as follows and the pressure along y coordinate can be obtained according to Eq. (6) then.

$$p = p_0 + \varepsilon p_1 + \varepsilon^2 p_2 + \dots = p_0 + \sum_{i=1}^{\infty} \varepsilon^i p_i \quad (11)$$

where p_0 denotes solution of the plate with constant thickness, p_i are solutions accounting for the thickness variation.

Substituting Eqs. (6), (8), (9) and (11) into Eq. (5), collecting the like terms in ε^0 , one can obtain

$$\Psi(w_0) = 0 \quad (12)$$

then collecting the like terms in $\varepsilon^i(i \geq 1)$, one obtains

$$\Psi(w_i) = -\frac{p_i a^2}{D_0} \frac{\partial^2 w_0}{\partial \xi^2} - \lambda \frac{p_i b^2}{D_0} \frac{\partial^2 w_0}{\partial \eta^2} + T_i \quad (13)$$

the operator Ψ is defined as

$$\Psi(w) = \frac{\partial^4 w}{\partial \xi^4} + 2 \frac{a^2}{b^2} \frac{\partial^4 w}{\partial \xi^2 \partial \eta^2} + \frac{a^4}{b^4} \frac{\partial^4 w}{\partial \eta^4} + \frac{p_0 a^2}{D_0} \frac{\partial^2 w}{\partial \xi^2} + \lambda \frac{p_0 b^2}{D_0} \frac{\partial^2 w}{\partial \eta^2} \quad (14)$$

Taking the like terms in ε for an example, the first term of T_i is provided as follows

$$\begin{aligned} T_1 &= -3H_1 \left(\frac{\partial^4 w_0}{\partial \xi^4} + 2 \frac{a^2}{b^2} \frac{\partial^4 w_0}{\partial \xi^2 \partial \eta^2} + \frac{a^4}{b^4} \frac{\partial^4 w_0}{\partial \eta^4} \right) \\ &\quad - 6 \frac{\partial H_1}{\partial \xi} \frac{\partial}{\partial \xi} \left(\frac{\partial^2 w_0}{\partial \xi^2} + \frac{a^2}{b^2} \frac{\partial^2 w_0}{\partial \eta^2} \right) - 6 \frac{a^2}{b^2} \frac{\partial H_1}{\partial \eta} \frac{\partial}{\partial \eta} \left(\frac{\partial^2 w_0}{\partial \xi^2} + \frac{a^2}{b^2} \frac{\partial^2 w_0}{\partial \eta^2} \right) \\ &\quad - 3 \frac{\partial^2 H_1}{\partial \xi^2} \left(\frac{\partial^2 w_0}{\partial \xi^2} + \frac{a^2}{b^2} \frac{\partial^2 w_0}{\partial \eta^2} \right) - 3 \frac{a^2}{b^2} \frac{\partial^2 H_1}{\partial \eta^2} \left(\frac{\partial^2 w_0}{\partial \xi^2} + \frac{a^2}{b^2} \frac{\partial^2 w_0}{\partial \eta^2} \right) \\ &\quad - 6(1-\nu) \frac{a^2}{b^2} \frac{\partial^2 H_1}{\partial \xi \partial \eta} \frac{\partial^2 w_0}{\partial \xi \partial \eta} \end{aligned} \quad (15)$$

The Eq. (12) will be solved firstly and the solution that satisfying the boundary condition is sought as

$$w_0 = A_{0mn} \sin m\pi\xi \sin n\pi\eta \quad (16)$$

where m and n are the half-wave numbers of the plate along x and y coordinates respectively, A_{0mn} is undetermined amplitude.

Substituting Eq. (16) into Eq. (12) yields

$$p_0 = \frac{D_0 \pi^2 \left(m^2 + \frac{a^2}{b^2} n^2 \right)^2}{a^2 m^2 + \lambda b^2 n^2} \quad (17)$$

For a rectangular plate with constant thickness under certain bi-axial compression, the critical buckling load p_{0cr} as well as the corresponding buckling mode (m, n) can be determined according to Eq. (17) by minimizing p_0 with various combination of m and n .

Then, the solution of Eq. (13) will be solved in the following form

$$w_i = \sum_{j=1}^{\infty} \sum_{k=1}^{\infty} A_{ijk} \sin j\pi\xi \sin k\pi\eta \quad (18)$$

where j and k are integers and A_{ijk} is undetermined amplitude.

Substituting Eq. (18) into Eq. (13), one can obtain

$$\begin{aligned} &\frac{p_i \pi^2}{D_0} \left(a^2 m^2 + \lambda b^2 n^2 \right) A_{0mn} \sin m\pi\xi \sin n\pi\eta + T_i \\ &= \sum_{j=1}^{\infty} \sum_{k=1}^{\infty} \left[\left[(j\pi)^2 + \frac{a^2}{b^2} (k\pi)^2 \right]^2 \right. \\ &\quad \left. - \frac{p_0 a^2}{D_0} (j\pi)^2 - \lambda \frac{p_0 b^2}{D_0} (k\pi)^2 \right] A_{ijk} \sin j\pi\xi \sin k\pi\eta \end{aligned} \quad (19)$$

Applying the Galerkin method, both sides of Eq. (19) will be multiplied by $\sin m\pi\xi \sin n\pi\eta$ and integrated to ξ and η from 0 to 1 respectively. We will obtain

$$\begin{aligned} & \frac{p_i \pi^2}{4D_0} (a^2 m^2 + \lambda b^2 n^2) A_{0mn} + \int_0^1 \int_0^1 T_i \sin m\pi\xi \sin n\pi\eta d\xi d\eta \\ &= \frac{A_{ijk}}{4} \left[\left[(m\pi)^2 + \frac{a^2}{b^2} (n\pi)^2 \right]^2 - \frac{p_0 a^2}{D_0} (m\pi)^2 - \lambda \frac{p_0 b^2}{D_0} (n\pi)^2 \right] \end{aligned} \quad (20)$$

According to Eq. (17), right side of Eq. (20) will become zero. Then, Eq. (20) can be transformed as

$$p_i = - \frac{4D_0 \int_0^1 \int_0^1 T_i \sin m\pi\xi \sin n\pi\eta d\xi d\eta}{A_{0mn} \pi^2 (a^2 m^2 + \lambda b^2 n^2)} \quad (21)$$

Thus, the asymptotic formula of the critical buckling load for the rectangular plate with arbitrary thickness variation under bi-axial compression can be given by

$$\begin{aligned} p_{cr} &= p_{0cr} + \sum_{i=1}^{\infty} \varepsilon^i p_i = \frac{D_0 \pi^2 \left(m^2 + \frac{a^2}{b^2} n^2 \right)^2}{a^2 m^2 + \lambda b^2 n^2} \\ &- \frac{4D_0}{A_{0mn} \pi^2 (a^2 m^2 + \lambda b^2 n^2)} \sum_{i=1}^{\infty} \varepsilon^i \int_0^1 \int_0^1 T_i \sin m\pi\xi \sin n\pi\eta d\xi d\eta \end{aligned} \quad (22)$$

Since the undetermined amplitude A_{0mn} is included in the T_i term, it will be eliminated automatically from Eq. (22) in the solving process. Then, Eq. (22) will be used to evaluate buckling behavior of thin rectangular plates with different geometries and different variable thicknesses under different forces.

3. Numerical analysis and validation

3.1 Case 1: Plate with linear and parabolic thickness variations along x coordinate

Eq. (23) as follows is used to describe the thickness variations which $\beta=1$ represents the linear form and $\beta=2$ represents the parabolic form. Cross-section of the plates with this two thickness variation forms have been shown in Fig. 2. h_0 is the nominal thickness at $x=0$ and h_e is the thickness at $x=a$.

$$h(x) = h_0 - (h_0 - h_e) \left(\frac{x}{a} \right)^\beta \quad (23)$$

According to Eq. (4), the non-dimensional form of Eq. (23) will be obtained as follows

$$H = 1 - \left(1 - \frac{h_e}{h_0} \right) \xi^\beta \quad (24)$$

in which $\varepsilon = 1 - h_e/h_0$, $H_1 = -\xi^\beta$ and $H_i (i \geq 2) = 0$.

Substituting Eq. (24) and relevant parameters into Eq. (22), the critical buckling load of the plate corresponding to linear and parabolic thickness variations can be obtained as follows

$\beta=1$:

$$p_{cr} = \frac{D_0 \pi^2}{a^2 m^2 + \lambda b^2 n^2} \left(m^2 + \frac{a^2}{b^2} n^2 \right)^2 \left(\frac{3h_e}{2h_0} - \frac{1}{2} \right) \quad (25)$$

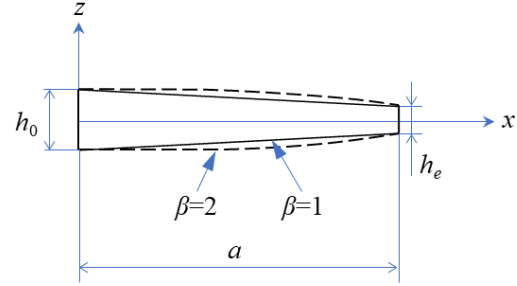


Fig. 2 Rectangular plate under biaxial compression

$\beta=2$:

$$\begin{aligned} p_{cr} &= \frac{D_0 \pi^2}{a^2 m^2 + \lambda b^2 n^2} \left(m^2 + \frac{a^2}{b^2} n^2 \right)^2 \\ &- \frac{D_0}{a^2 m^2 + \lambda b^2 n^2} \left(1 - \frac{h_e}{h_0} \right) \left[\left(\pi^2 - \frac{3}{2m^2} \right) \left(m^2 + \frac{a^2}{b^2} n^2 \right)^2 \right. \\ &\quad \left. + 6 \frac{a^2}{b^2} n^2 (1 - \nu) \right] \end{aligned} \quad (26)$$

The critical buckling load p_{cr} will be transformed into non-dimensional form by introducing a critical buckling factor φ as

$$\varphi = \frac{p_{cr} b^2}{\pi^2 D_0} \quad (27)$$

The critical buckling factor of the plates with different thickness variation amplitudes $h_0/h_e = 1.125, 1.25, 1.375, 1.5$ under bi-axial compression are shown in Tables 1-3. The Poisson's ratio is taken as $\nu=0.3$. Buckling mode is given next to the value of the plate's aspect ratio in the Tables 1-3.

For verification, the available results from Eisenberger and Alexandrov (2003) are compared with the current results obtained from this paper in Tables 4 and 5. Since the critical buckling load in Eisenberger and Alexandrov (2003) is normalized as $\varphi' = p_{cr} b^2 / \pi^2 D_e$ where $D_e = Eh_e^3 / 12(1 - \nu^2)$ and the Poisson's ratio is taken as 0.25 which are different from this paper, the results obtained in Tables 1-3 will be transformed according to Eisenberger and Alexandrov (2003) for comparison as shown in Tables 4 and 5. Similarly, the available results from Chehil and Dua (1973) are compared in Tables 6. The flexural rigidity D_{av} in Chehil and Dua (1973) was defined as $Eh_{av}^3 / 12(1 - \nu^2)$, where $h_{av} = (h_0 + h_e)/2$ in this paper. Besides, the Poisson's ratio was taken as 1/3 which is also different from this paper. So, the results in Table 1 will be transformed according to Chehil and Dua (1973) for comparison as shown in Tables 6.

It can be seen from Tables 4-6 that the critical buckling loads obtained by the method in this paper are in close agreement with that in Eisenberger and Alexandrov (2003) and Chehil and Dua (1973) for different aspect ratios and thickness variation amplitudes, which verifies the method presented in this paper. Based on that, the variation of critical buckling factors with thickness variation amplitude for the plates with different aspect ratios at $\lambda=1$ are shown in Figs. 3 and 4 which representing the linear and parabolic thickness variations respectively.

Table 1 Critical buckling factor φ for $\lambda=0$

a/b	$\beta=1$ h_0/h_e				$\beta=2$ h_0/h_e			
	1.125	1.25	1.375	1.5	1.125	1.25	1.375	1.5
0.25(1,1)	15.05	12.64	10.67	9.03	16.31	14.91	13.77	12.81
0.5(1,1)	5.21	4.38	3.69	3.13	5.61	5.1	4.69	4.34
1(1,1)	3.33	2.8	2.36	2	3.58	3.24	2.96	2.73
2(2,1)	3.33	2.8	2.36	2	3.56	3.21	2.92	2.68
3.5(4,1)	3.39	2.85	2.41	2.04	3.62	3.26	2.96	2.72
5(5,1)	3.33	2.8	2.36	2	3.56	3.2	2.91	2.67

Table 2 Critical buckling factor φ for $\lambda=0.5$

a/b	$\beta=1$ h_0/h_e				$\beta=2$ h_0/h_e			
	1.125	1.25	1.375	1.5	1.125	1.25	1.375	1.5
0.25(1,4)	0.41	0.35	0.29	0.25	0.44	0.4	0.37	0.34
0.5(1,2)	1.48	1.24	1.05	0.89	1.59	1.44	1.32	1.21
1(1,1)	2.22	1.87	1.58	1.33	2.38	2.16	1.97	1.82
2(2,1)	3.23	2.72	2.29	1.94	3.45	3.11	2.83	2.6
3.5(4,1)	3.38	2.84	2.4	2.03	3.61	3.25	2.96	2.71
5(5,1)	3.33	2.8	2.36	2	3.55	3.2	2.91	2.66

Table 3 Critical buckling factor φ for $\lambda=1$

a/b	$\beta=1$ h_0/h_e				$\beta=2$ h_0/h_e			
	1.125	1.25	1.375	1.5	1.125	1.25	1.375	1.5
0.25(1,4)	0.21	0.17	0.15	0.12	0.22	0.2	0.18	0.17
0.5(1,2)	0.78	0.66	0.56	0.47	0.84	0.76	0.7	0.64
1(1,1)	1.67	1.4	1.18	1	1.79	1.62	1.48	1.36
2(2,1)	3.14	2.64	2.22	1.88	3.35	3.02	2.75	2.52
3.5(4,1)	3.38	2.84	2.39	2.03	3.6	3.24	2.95	2.7
5(5,1)	3.33	2.8	2.36	2	3.55	3.2	2.91	2.66

Table 4 Comparison of critical buckling factors φ' for linear thickness variation $\beta=1$ ($\varphi'=p_{cr}b^2/\pi^2D_e$)

φ'	$a/b=0.5$ h_0/h_e		$a/b=2$ h_0/h_e	
	1.125	1.25	1.125	1.25
Eisenberger and Alexandrov (2003)	7.4678	8.7769	4.6295	5.1138
Present	7.4181	8.5547	4.7413	5.4688

Table 5 Comparison of critical buckling factors φ' for parabolic thickness variation $\beta=2$ ($\varphi'=p_{cr}b^2/\pi^2D_e$)

φ'	$a/b=0.5$ h_0/h_e		$a/b=1$ h_0/h_e		$a/b=2$ h_0/h_e	
	1.125	1.25	1.125	1.25	1.125	1.25
Eisenberger and Alexandrov (2003)	7.9879	9.9550	5.0655	6.2174	4.9015	5.6685
Present	7.9883	9.9586	5.0865	6.3094	5.0685	6.2648

Table 6 Comparison of critical buckling factors φ' for linear thickness variation $\beta=1$ ($\varphi'=p_{cr}b^2/\pi^2D_{av}$)

φ'	$a/b=0.25$ h_0/h_e			$a/b=0.5$ h_0/h_e			$a/b=1$ h_0/h_e		
	1.125	1.25	1.375	1.125	1.25	1.375	1.125	1.25	1.375
Chehil and Dua (1973)	17.990	17.803	17.538	6.225	6.160	6.068	3.966	3.878	3.753
Present	17.451	16.937	16.180	6.041	5.869	5.596	3.861	3.752	3.579

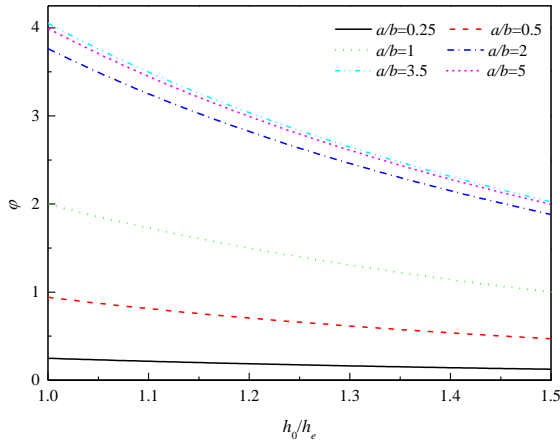


Fig. 3 Critical buckling factor vs thickness variation amplitude when $\beta=1$

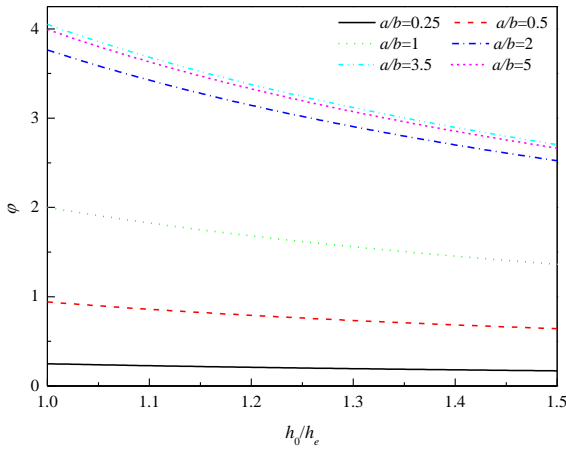


Fig. 4 Critical buckling factor vs thickness variation amplitude when $\beta=2$

As it can be seen that the critical buckling factor φ will decrease as the thickness variation amplitude h_0/h_e increases. For the plate with larger aspect ratio, the critical buckling factor is higher and effects of thickness variation on the critical buckling factor are greater. Comparison between Fig. 3 and Fig. 4 shows that reduction amplitude of the critical buckling factor as h_0/h_e increases is relatively larger for $\beta=1$. It means that linear thickness variation has greater influence on buckling behavior of the rectangular plate than the parabolic thickness variation.

3.2 Case 2: Plate with stepped thickness variation along x coordinate

The stepped thickness variation form as shown in Fig. 5 can be expressed by Eq. (28), in which K is the auxiliary parameter that tends to be infinite. Taking the plate with $h_{10}/h_{20}=1.5$ and $a_1/a=0.4$ as an example, the schematic diagram of the plate's thickness that expressed by Eq. (28) is shown in Fig. 6.

$$h(x) = \frac{h_{10} + h_{20}}{2} - \frac{h_{10} - h_{20}}{\pi} \arctan K(x - a_1) \quad (28)$$

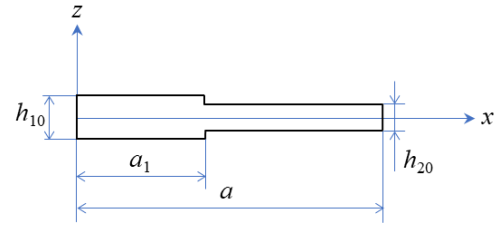


Fig. 5 Stepped thickness variation form

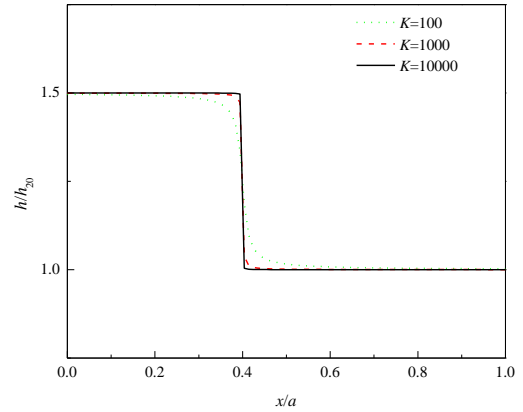


Fig. 6 Description of stepped thickness variation by Eq. (28)

It can be seen from Fig. 6 that as the auxiliary parameter K becomes larger gradually, the thickness variation tends to be the stepped pattern. When K reaches 10000, the wall thickness curve in Fig. 6 can describe the thickness variation of the plate quite accurately.

Eq. (28) will be transformed into non-dimensional form as follows

$$H = 1 - \varepsilon \arctan Ka \left(\xi - \frac{a_1}{a} \right) \quad (29)$$

where

$$h_0 = \frac{h_{10} + h_{20}}{2}, \quad \varepsilon = \frac{2(h_{10} - h_{20})}{\pi(h_{10} + h_{20})}, \quad H_1 = -\arctan Ka \left(\xi - \frac{a_1}{a} \right) \quad (30)$$

Substituting Eq. (29) and Eq. (30) into Eq. (22), the critical buckling load of the plate with stepped thickness variation can be obtained as follows

$$p_{cr} = \frac{D_0 \pi^2}{a^2 m^2 + \lambda b^2 n^2} \left(m^2 + \frac{a^2}{b^2} n^2 \right)^2 \times \left\{ 1 - \frac{3(h_{10} - h_{20})}{\pi m(h_{10} + h_{20})} \left[\sin \left(2\pi \frac{a_1}{a} m \right) + \pi m \left(1 - 2 \frac{a_1}{a} \right) \right] \right\} \quad (31)$$

Similarly, Eq. (31) will be transformed into non-dimensional form by introducing the critical buckling factor as

$$\varphi = \frac{p_{cr} b^2}{\pi^2 D_{10}} \quad (32)$$

Table 7 Critical buckling factor φ for $\lambda=0$

a/b	$a_1/a=0.2$			$a_1/a=0.4$			$a_1/a=0.6$			$a_1/a=0.8$		
	h_{10}/h_{20}			h_{10}/h_{20}			h_{10}/h_{20}			h_{10}/h_{20}		
	1.25	1.5	1.75	1.25	1.5	1.75	1.25	1.5	1.75	1.25	1.5	1.75
0.25(1,1)	9.21	4.79	2.29	11.47	8.03	5.99	14.87	12.88	11.54	17.13	16.11	15.32
0.5(1,1)	3.19	1.66	0.79	3.97	2.78	2.07	5.14	4.46	3.99	5.93	5.58	5.27
1(1,1)	2.04	1.06	0.51	2.54	1.78	1.33	3.29	2.85	2.55	3.79	3.57	3.37
2(2,1)	2.24	1.35	0.84	2.87	2.25	1.86	2.96	2.38	2.02	3.59	3.28	3.04
3.5(4,1)	2.45	1.62	1.13	2.82	2.14	1.73	3.12	2.57	2.22	3.49	3.1	2.82
5(5,1)	2.33	1.48	0.99	2.72	2.04	1.62	3.11	2.59	2.26	3.5	3.15	2.89

Table 8 Critical buckling factor φ for $\lambda=0.5$

a/b	$a_1/a=0.2$			$a_1/a=0.4$			$a_1/a=0.6$			$a_1/a=0.8$		
	h_{10}/h_{20}			h_{10}/h_{20}			h_{10}/h_{20}			h_{10}/h_{20}		
	1.25	1.5	1.75	1.25	1.5	1.75	1.25	1.5	1.75	1.25	1.5	1.75
0.25(1,4)	0.25	0.13	0.06	0.32	0.22	0.16	0.41	0.35	0.32	0.47	0.44	0.42
0.5(1,2)	0.91	0.47	0.23	1.13	0.79	0.59	1.46	1.27	1.14	1.69	1.59	1.5
1(1,1)	1.36	0.71	0.34	1.69	1.18	0.88	2.19	1.9	1.7	2.53	2.38	2.25
2(2,1)	2.17	1.31	0.81	2.78	2.18	1.81	2.87	2.31	1.96	3.48	3.18	2.95
3.5(4,1)	2.44	1.61	1.12	2.81	2.13	1.72	3.11	2.57	2.22	3.48	3.09	2.82
5(5,1)	2.33	1.48	0.99	2.72	2.04	1.62	3.11	2.59	2.26	3.5	3.15	2.89

Table 9 Critical buckling factor φ for $\lambda=1$

a/b	$a_1/a=0.2$			$a_1/a=0.4$			$a_1/a=0.6$			$a_1/a=0.8$		
	h_{10}/h_{20}			h_{10}/h_{20}			h_{10}/h_{20}			h_{10}/h_{20}		
	1.25	1.5	1.75	1.25	1.5	1.75	1.25	1.5	1.75	1.25	1.5	1.75
0.25(1,4)	0.13	0.07	0.03	0.16	0.11	0.08	0.2	0.18	0.16	0.24	0.22	0.21
0.5(1,2)	0.48	0.25	0.12	0.6	0.42	0.31	0.77	0.67	0.6	0.89	0.84	0.79
1(1,1)	1.02	0.53	0.25	1.27	0.89	0.66	1.65	1.43	1.28	1.9	1.78	1.69
2(2,1)	2.11	1.27	0.79	2.7	2.12	1.75	2.79	2.24	1.9	3.38	3.09	2.86
3.5(4,1)	2.44	1.61	1.12	2.8	2.13	1.72	3.1	2.56	2.21	3.47	3.08	2.81
5(5,1)	2.33	1.48	0.99	2.72	2.03	1.62	3.11	2.59	2.25	3.49	3.14	2.89

Table 10 Comparison of critical buckling factors φ' for $\lambda=0$ and $a/b=1$ ($\varphi'=p_{cr}b^2/\pi^2D_{20}$)

a_1/a	h_{10}/h_{20}	Xiang and Wang (2002)	Present
0.3	1.2	4.5131	4.7280
	1.5	5.1516	5.3884
0.7	1.2	5.7436	5.8694
	1.5	7.6886	7.8731

The critical buckling factor of the plates with different thickness variation amplitudes $h_{10}/h_{20} = 1.25, 1.5, 1.75$ and different stepped lengths $a_1/a=0.2, 0.4, 0.6, 0.8$ under bi-axial compression are shown in Tables 7-9. Buckling mode is also given next to the value of the plate's aspect ratio in these tables.

In order to verify the presented method, the available results from Xiang and Wang (2002) and Wilson and Rajasekaran (2014) are compared with the results obtained from this paper in Tables 10 and 11. Because the critical

buckling load in the above references is normalized as $\varphi'=p_{cr}b^2/\pi^2D_{20}$ and the Poisson's ratio is taken as 0.25, the results obtained in this paper will be transformed according to that as shown in Tables 10 and 11.

It can be seen from Tables 10 and 11 that the results obtained by present analysis are in close agreement with the previous work. It verifies the accuracy of the present theoretical method. According to the numerical results, the variation of critical buckling factors with thickness variation amplitude for the plates with different aspect

Table 11 Comparison of critical buckling factors φ' for $\lambda=1$ and $a/b=1$ ($\varphi'=p_{cr}b^2/\pi^2D_{20}$)

a_1/a	h_{10}/h_{20}	Xiang and Wang (2002)	Wilson and Rajasekaran (2014)	Present
0.3	1.2	2.2867	2.9547	2.3640
	1.5	2.7171	2.7444	2.9442
	2.0	3.4449	3.4971	3.9793
0.7	1.2	2.9547	2.9471	2.9347
	1.5	4.4051	4.4295	4.7865
	2.0	6.6870	6.8006	6.9852

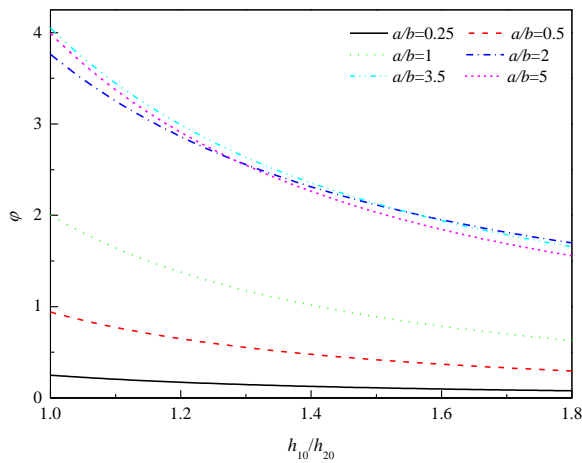


Fig. 7 Critical buckling factor vs thickness variation amplitude when $a_1/a=0.4$

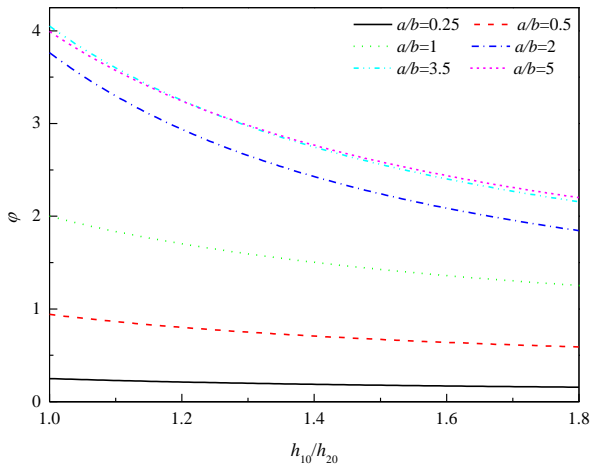


Fig. 8 Critical buckling factor vs thickness variation amplitude when $a_1/a=0.6$

ratios at $\lambda=1$ are shown in Figs. 7 and 8 corresponding to $a_1/a=0.4$ and 0.6 respectively.

As it can be seen from Figs. 7 and 8, the critical buckling factor for the plate with larger aspect ratio is bigger than that with smaller aspect ratio. Effects of thickness variation on bucking behavior of stepped plates are greater for the larger aspect ratios, and as the stepped length a_1/a increases, the effects will become smaller.

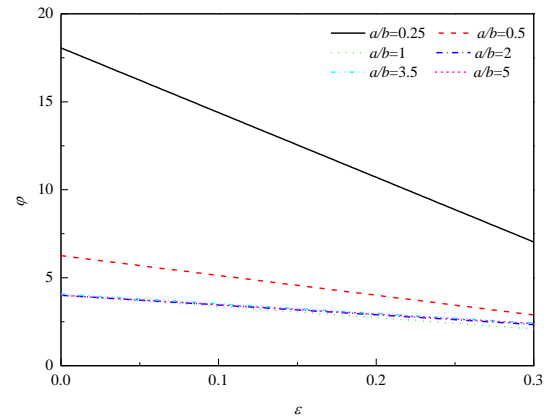


Fig. 9 Critical buckling factor vs thickness variation amplitude when $\lambda=0$

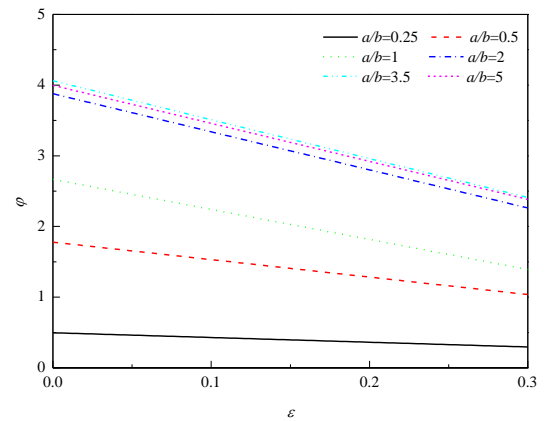


Fig. 10 Critical buckling factor vs thickness variation amplitude when $\lambda=0.5$

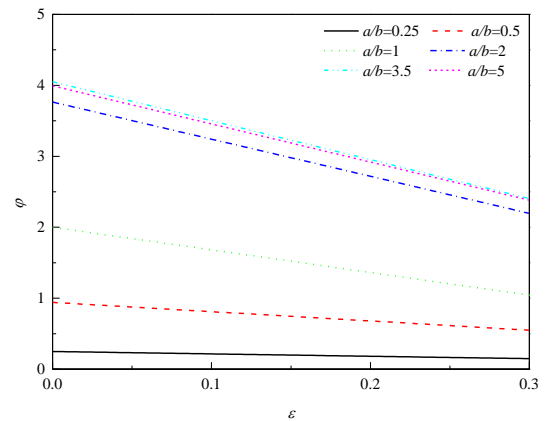


Fig. 11 Critical buckling factor vs thickness variation amplitude when $\lambda=1$

3.3 Case 3: Plate with trigonometric thickness variation along x and y coordinates

The thickness expression of rectangular plate with trigonometric thickness variation along both x and y coordinates has been shown in Eq. (33).

$$h(x, y) = h_0 \left(1 - \varepsilon \sin \pi \frac{x}{a} \sin \pi \frac{y}{b} \right) \quad (33)$$

ε is the non-dimensional parameter indicating the thickness variation magnitude defined in Eq. (7) satisfying $0 \leq \varepsilon \leq 1$. It will be transformed into non-dimensional form as follows

$$H = 1 - \varepsilon \sin \pi \xi \sin \pi \eta \quad (34)$$

Taking $\varepsilon=0.2$ as an example, the Eq. (34) and relevant parameters is substituted into Eq. (22), the critical buckling load of the plate with trigonometric thickness variation can be obtained as follows

$$P_{cr} = \frac{D_0 \pi^2 \left(m^2 + \frac{a^2}{b^2} n^2 \right)^2}{a^2 m^2 + \lambda b^2 n^2} - \frac{192 D_0 m^2 n^2}{(4m^2 - 1)(4n^2 - 1)(a^2 m^2 + \lambda b^2 n^2)} \times \left[\left(m^2 + \frac{a^2}{b^2} n^2 \right)^2 + \left(1 + \frac{a^2}{b^2} v \right) m^2 + \left(v \frac{a^2}{b^2} + \frac{a^4}{b^4} \right) n^2 + \frac{(1-v)a^2}{2b^2} - \left(1 + \frac{a^2}{b^2} \right) \left(m^2 + \frac{a^2}{b^2} n^2 \right) \right] \varepsilon \quad (35)$$

According to Eq. (27), critical buckling factor of the plates with trigonometric thickness variation will be obtained by transforming Eq. (34) into non-dimensional form. The variation of critical buckling factor φ with thickness variation amplitude ε for the plates with different aspect ratios at $\lambda=0$, $\lambda=0.5$, $\lambda=1$ are shown in Figs. 9-11 respectively.

As we can see, the critical buckling factor decreases gradually as the thickness variation amplitude increases. It verifies that the buckling capacity of the plate will be weakened because of the thickness reduction. Eq. (34) and Figs 9-11 can be used as references to obtain the critical buckling load of different rectangular plates with trigonometric thickness variation.

5. Conclusions

Combining the perturbation technique, Fourier series expansion and Galerkin methods, the linear governing differential equation of the simply supported plate with arbitrary thickness variation under bi-axial compression is solved. The analytical formulas of critical buckling loads and buckling modes have been established. Numerical analyses on the critical buckling loads of the plates with different thickness variation forms including linear, parabolic, stepped and trigonometric under different load combinations are presented. Comparative analysis with previous work has also been carried out. It shows that the critical buckling loads calculated by the method in this paper coincide well with the available references, which verifies the accuracy of the presented method. Numerical analyses reveal that the analytical formulas derived in this paper can be used to calculate critical buckling load and evaluate buckling capacity of the variable thickness plates conveniently and efficiently. Results show that different thickness variation forms have different effects on buckling behavior of the simply supported plates under bi-axial compression. For the plates with linear and parabolic thickness variations, the detrimental effects of thickness reduction on the buckling capacity are more serious for the

plates with linear thickness variation and larger aspect ratio. For the plates with stepped thickness variation, the detrimental effects are greater for the smaller stepped length a_1/a and larger aspect ratios. For the plates with trigonometric variable thickness, increase of thickness variation amplitude will make them more vulnerable to buckling. The analytical method presented in this paper can be used as reference for buckling analysis and design of simply supported thin variable thickness plates under bi-axial compression.

Acknowledgments

The research described in this paper was financially supported by the Fundamental Research Funds for the Central Universities (No. DUT19JC19 and No. DUT17JC18) and the Project funded by China Postdoctoral Science Foundation (No. 2019M651112).

References

- Azhari, M., Shahidi, A.R. and Saadatpour, M.M. (2005), "Local and post local buckling of stepped and perforated thin plates", *Appl. Math. Model.*, **29**(7), 633-652.
- Chehil, D.S. and Dua S.S. (1973), "Buckling of rectangular plates with general variation in thickness", *J. Appl. Mech.-T. ASME*, **40**(3), 745-751.
- Chen, L., Rotter, J.M. and Doerich-Stavridis, C. (2012), "Practical calculations for uniform external pressure buckling in cylindrical shells with stepped walls", *Thin Wall. Struct.*, **61**, 162-168.
- Eisenberger, M. and Alexandrov, A. (2003), "Buckling loads of variable thickness thin isotropic plates", *Thin Wall. Struct.*, **41**(9), 871-889.
- Gong, J., Tao, J., Zhao, J., Zeng, S. and Jin, T. (2013), "Buckling analysis of open top tanks subjected to harmonic settlement", *Thin Wall. Struct.*, **63**, 37-43.
- Kobayashi, H. and Sonoda, K. (1990), "Buckling of rectangular plates with tapered thickness", *J. Struct. Eng.-ASCE*, **116**(5), 1278-1289.
- Li, R., Zheng, X., Wang, H., Xiong, S., Yan, K. and Li, P. (2018), "New analytic buckling solutions of rectangular thin plates with all edges free", *Int. J. Mech. Sci.*, **144**, 67-73.
- Minh, P.P., Van Do, T., Duc, D.H. and Nguyen, D.D. (2018), "The stability of cracked rectangular plate with variable thickness using phase field method", *Thin Wall. Struct.*, **129**, 157-165.
- Navaneethakrishnan, P.V. (1988), "Buckling of nonuniform plates: spline method", *J. Eng. Mech.-ASCE*, **114**(5), 893-898.
- Nerantzaki, M.S. and Katsikadelis, J.T. (1996), "Buckling of plates with variable thickness—an analog equation solution", *Eng. Anal. Bound. Elem.*, **18**(2), 149-154.
- Rajasekaran, S. and Wilson, A. J. (2013), "Buckling and vibration of rectangular plates of variable thickness with different end conditions by finite difference technique", *Struct. Eng. Mech.*, **46**(2), 269-294.
- Saeidifar, M., Sadeghi, S.N. and Sayiz, M.R. (2010), "Analytical solution for the buckling of rectangular plates under uni-axial compression with variable thickness and elasticity modulus in the y-direction", *P. I. Mech. Eng. C-J. Mec.*, **224**(1), 33-41.
- Wang, B., Li, P. and Li, R. (2016), "Symplectic superposition method for new analytic buckling solutions of rectangular thin plates", *Int. J. Mech. Sci.*, **119**, 432-441.
- Wang, X., Wang, Y. and Ge, L. (2016), "Accurate buckling

- analysis of thin rectangular plates under locally distributed compressive edge stresses", *Thin Wall. Struct.*, **100**, 81-92.
- Wilson, A.J. and Rajasekaran, S. (2013), "Elastic stability of all edges clamped stepped and stiffened rectangular plate under uni-axial, bi-axial and shearing forces", *Meccanica*, **48**(10), 2325-2337.
- Wilson, A.J. and Rajasekaran, S. (2014), "Elastic stability of all edges simply supported, stepped and stiffened rectangular plate under Biaxial loading", *Appl. Math. Model.*, **38**(2), 479-495.
- Wittrick, W.H. and Ellen, C.H. (1962), "Buckling of tapered rectangular plates in compression", *Ae. Q.*, **13**(4), 308-326.
- Xiang, Y. and Wang, C.M. (2002), "Exact buckling and vibration solutions for stepped rectangular plates", *J. Sound Vib.*, **250**(3), 503-517.
- Xiang, Y. and Wei, G.W. (2004), "Exact solutions for buckling and vibration of stepped rectangular Mindlin plates", *Int. J. Solids Struct.*, **41**, 279-294.